



Radar Pulse Compression with Optimized Weighting Window for SAR Receivers

Khalid F. A. Hussein¹ · Asmaa O. Helmy³ · Ashraf S. Mohra²

Accepted: 7 May 2022
© The Author(s) 2022

Abstract

This paper proposes a novel design of a software-defined matched filter (MF) for digital receivers of synthetic aperture radar (SAR). The block diagram of the proposed receiver is described in detail. The purpose of this filter is to produce a SAR pulse with higher compression ratio (CR) and lower side lobe level (SLL) than that produced by the conventional MF. The proposed design is based on the idea of time windowing of the SAR pulse to construct the transfer function of the receiver filter. The shape of the proposed time-domain window is optimized to achieve the filter design goals including the minimization of the SLL and the realization of the target value of the CR. The transmitted SAR pulse is, first, subjected to linear frequency modulation and then subjected to the optimized window. The width (time duration) of the proposed window is divided into equal time intervals. The proposed time-domain window is constructed as a sequential continuous piecewise linear segments. The instantaneous value of the time-domain window at the start of each time interval is optimized so as to achieve the optimization goals. The width of the time-domain window is shown to be proportional to the width of the compressed pulse after optimization. The number of the time intervals into which the time duration of the window is divided is shown to have a significant effect on the optimization results. The particle swarm optimization (PSO) technique is then applied to get the window shape that minimizes the SLL for a specific predetermined value of the pulse CR. It is shown that the iterations of the PSO are fastly convergent and that the applied algorithm is computationally efficient. Also, it is shown that the desired value of the pulse CR is achieved with accuracy of 100%. Moreover, the achieved SLLs are about -65 dB, -90 dB, -114 dB, and -133 dB for pulse CR of 5, 3, 2, and 1.5, respectively. Finally, for practical implementation of the introduced SAR pulse processing technique, the proposed optimized window is placed as a building block in a software-defined receiver of the SAR system.

Keywords Pulse compression · Software defined receiver · Linear frequency modulation (LFM) · Particle swarm optimization algorithm (PSO)

✉ Khalid F. A. Hussein
fkhalid@eri.sci.eg; khalid_elgabaly@yahoo.com

Extended author information available on the last page of the article

1 Introduction

Synthetic aperture radar (SAR) can be considered as the most effective land imaging system for earth remote sensing irrespective of the daytime and environmental conditions [1–4]. High imaging resolution and high performance of land target detection are essential requirements for efficient SAR systems [5]. Thus, in the design of SAR system transceiver, the main concern is the imaging resolution and the performance of land target detection. In pulsed SAR systems, a short pulse is required for high image resolution whereas a long pulse is required for high detection performance [5]. Consequently, there is always a trade-off between imaging resolution and detection performance. In this context, SAR pulse compression techniques are adapted to mitigate this trade-off problem by gathering some benefits of both high resolution and detection-performance. In pulse compression techniques, the transmitted SAR pulse has longer duration for high detection performance whereas its bandwidth corresponds to a shorter pulse to achieve high imaging resolution; see Fig. 1.

One of the most important issues in the SAR system design is the software-defined SAR transceiver design [6–10]. In a typical SAR receiver that employs frequency chirping for pulse compression, the received SAR echo is processed using a matched filter (MF) to get its time-domain form at the MF output as a pulse that has a main lobe and multiple sidelobes. The matched filter of the SAR receiver maximizes the signal-to-noise ratio at the receiver output leading to increase the receiver sensitivity and, thus, enhancing the radar system performance. Moreover, for a compressed SAR pulse by applying frequency chirping, the MF leads to suppress the sidelobe level of the received SAR echo at the receiver output and, thus, improves the SAR imaging resolution.

Satisfactory design of the frequency chirping of the transmitted pulse results in a received echo pulse with a main lobe of much higher level than that of the side lobes. Also, the width of the main lobe is much narrower than that of the transmitted pulse. The width of the received echo pulse at the MF output can be calculated as the time difference between the first two nulls on the sides of the main lobe of the signal at the MF output. For satisfactory performance of the operation of SAR pulse compression, it is required to get a pulse compression ratio (CR) that is equal to a predetermined (desired) value. The CR can

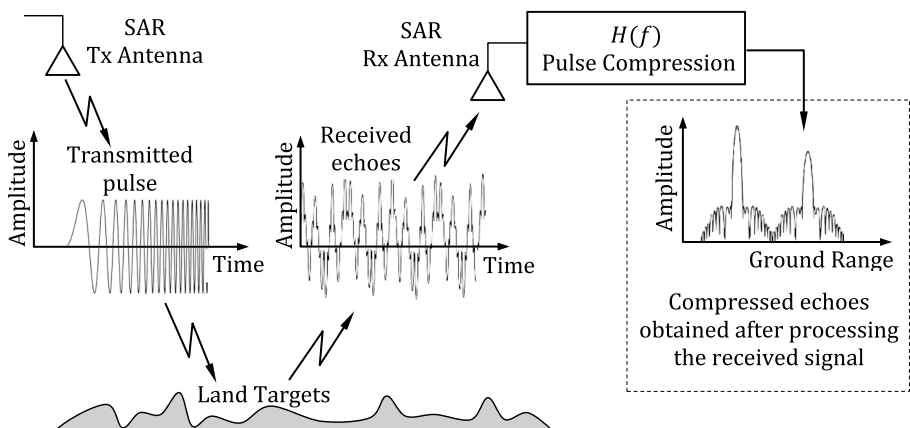


Fig. 1 Scheme of SAR pulse compression for enhancing the imaging resolution

be defined as the ratio between the width of the main lobe of the received signal at the MF output and the width of the transmitted pulse before chirping.

Over the last decade, a lot of research works have been concerned with issue of SAR pulse compression. For example, the work of [9] proposes a radar pulse compression scheme through an approach that is related to the design of efficient non-linear frequency modulation (NLFM) waveforms namely, a temporal predistortion method of LFM signals by some nonlinear frequency laws. This method produces a compressed radar pulse with SLL of about -40 dB. In [10], standard tapered windows are modified and applied to side lobe suppression in compressed pulses with LFM chirping to produce a compressed radar pulse with maximum SLL of about -43 dB. In [11], side lobe suppression is performed by some NLFM laws achieved by applying of a stationary phase technique (SPT) synthesis algorithm, where a SLL of about. In [12], different types of weighting window are applied for SLL reduction. This work demonstrates some important numerical results for the achieved SLL for the applied weighting windows of different shapes to show that triangular, Gaussian and Hann give the highest performance. In [13], stretch and correlation processing techniques are applied for pulse compression to achieve a highly compressed pulse, however, the achieved maximum SLL is about -23.8 dB. In [14], a variety of adaptive processing techniques are applied to range compression in SAR image focusing and evaluated under real and ideal conditions. Some research work present combined techniques for radar pulse compression. For example, in [15], the SAR pulse compression is performed using spectrum modification and window weighting technique. The application of such a combined technique is shown to be capable of reducing the maximum SLL to about -49 dB. The work of [16] introduces combination of phase predistortion and spectrum modification for SAR pulse compression to obtain a maximum SLL of about -62 dB.

In the present work, a novel design of the MF is proposed for the receiver of SAR to produce a SAR pulse with high CR and low SLL. The proposed MF design employs time windowing of the SAR pulse to construct the transfer function of the receiver filter. The time waveform of the proposed compression window is optimized to achieve the filter design goals including minimization of the SLL and realization of the desired CR. The proposed compression window is placed as a building block in a software defined receiver of the SAR system. The proposed pulse compression process requires the transmitted SAR pulse to be subjected to LFM. The time-domain window is constructed as a sequential continuous piecewise linear segments. The particle swarm optimization (PSO) [17] technique is then applied to get the window shape that minimizes the SLL for a specific target value of the CR.

The PSO is an evolutionary multi-objective optimization technique that can arrive at the best shape of the compression window so as to efficiently satisfy the multiple optimization goals including the minimization of the SLL and the achievement of a specific SAR pulse compression ratio. It can operate with small or large number control parameters even when they have inhomogeneous types. Moreover, the PSO is a simple, computationally efficient, and robust iterative technique that can arrive at the design goals even when the initial values of the control parameters are far from the optimum values. Owing to its fast convergence, the PSO algorithm can arrive at the design goals in a small number of iterations. Among the other evolutionary optimization technique, the PSO can be considered as the most effective and efficient technique for optimizing the shape of the compression window.

The remaining of this paper is organized as follows. The next section gives a mathematical formulation of the frequency chirping of SAR pulse. Section 3 provides a description of the conventional MF receiver used in the SAR system receiver for pulse compression. Section 4 gives a detailed description of the novel SAR system receiver proposed in the

present work with the optimized compression window. Section 5 explains how the PSO algorithm is applied to construct the time-domain compression window. Section 6 presents the numerical results with interesting discussions and conclusions. Finally, Sect. 7 summarizes the most important conclusions of the present work.

2 Frequency Chirping of the SAR Pulse

A conventional method for radar pulse compression is by frequency chirping using LFM. In LFM [5, 6], the radar pulse is constructed as a sinusoidal signal whose amplitude is constant over the pulse duration and zero otherwise. The frequency of the sinusoidal signal is f_b at the start of radar pulse and increases linearly with the time until it reaches f_e at the end time of the pulse. If the pulse duration is T then the slope of increase of the instantaneous frequency is $(f_e - f_b)/T$.

2.1 Time Waveform of the LFM Chirped Pulse

In LFM, the transmitted signal is a chirped pulse that can be expressed as follows.

$$s(t) = \sin\theta(t) \quad (1)$$

where $\theta(t)$ is the instantaneous value of the angle.

The instantaneous frequency, $f_i(t)$ can be obtained by differentiating $\theta(t)$ with respect to the time

$$f_i(t) = \frac{1}{2\pi} \frac{\partial\theta(t)}{\partial t} \quad (2)$$

To obtain LFM chirping the instantaneous frequency, $f_i(t)$, should take the following form

$$f_i(t) = \frac{(f_e - f_b)}{T} (t - t_b) + f_b, \quad t_b \leq t \leq t_e \quad (3)$$

where t_b is the start time of the pulse and $t_e = T + t_b$ is the end time of the pulse; f_b and f_e are the start and stop frequencies.

Thus, the angle $\theta(t)$ can be expressed as $\theta(t) = \int f_i(t) dt$; this gives,

$$\theta(t) = \frac{1}{2} \frac{(f_e - f_b)}{T} (t - t_b)^2 + f_b (t - t_b), \quad t_b \leq t \leq t_e \quad (4)$$

It should be noticed that constant of integration in (4) is set to get the phase angle of the sinusoidal signal equal to zero at the start of the pulse.

2.2 Time Discretization for Simulation

For simulation of the SAR pulse transmission, reception, and processing, the time should be discretized so as to apply fast Fourier transform (FFT) and inverse fast Fourier transform (IFFT) operations. Let N_s be the number of time samples of the transmitted SAR pulse, $s(t)$. Let the time interval between the successive samples be Δt . Thus, the start time

of the n th period is $t_n = (n - 1)\Delta t + t_b$ and $t_b = (n_b - 1)\Delta t$, where n_b is the number of the time sample at which the transmitted pulse starts. Thus, The total time for simulation is $T_T = L\Delta t$ where L is the total number of sampling periods over which the simulation is performed. The center frequency, $f_c = (f_b + f_e)/2$, is the operating frequency of the SAR. The bandwidth of operation is $B = f_e - f_b$, then the start and stop frequencies f_b, f_e can be, respectively, expressed as follows.

$$f_b = f_c - \frac{B}{2}, f_e = f_{N_s} = f_c + \frac{B}{2} \tag{5}$$

Thus, the n th frequency components of the transmitted pulse can be expressed as,

$$f_n = f_b + (n - 1)\Delta f; \Delta f = \frac{L}{\Delta t} \tag{6}$$

For accurate simulation, the sampling frequency, f_s , should be much greater than the center frequency f_c , i.e. $f_s \gg f_c$. The minimum sampling frequency $f_{s\min} = 2f_e$.

3 Conventional Design of the MF Receiver for SAR Pulse Compression

When the transmitted pulse travels from the SAR antenna to the target and is reflected back to the antenna it gets affected by noise. The main role of the MF [5, 6] is to efficiently retrieve the known transmitted signal from the received noisy signal, so MF-based receiver, the system is designed to search for the signal which has the similar characteristics as the transmitted pulse, in the received signal. The MF is an optimal filter which maximizes the signal to noise ratio (SNR) at the receiver output.

3.1 Conventional Design of MF Receiver for SAR Systems Employing FM Chirping

The transfer function of the MF can be described by the frequency response $H(f)$. A software-defined SAR receiver has its all functionalities applicable as software modules except for the low-noise amplifier (LNA). Such a receiver is shown in Fig. 2; the received echo is fed into a MF whose transfer function is the conjugate of the transmitted signal, $H(f) = S^*(f)$. The signal, $P(f)$, at the output of the MF is the compressed pulse which is the IFFT of the product of the received signal spectrum, $R(f)$, and the transfer function of the MF, $H(f)$. Thus, the signal spectrum at the MF output can be expressed as,

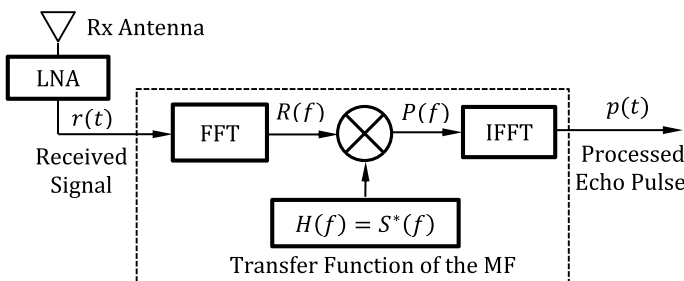


Fig. 2 Block diagram of the conventional software-defined MF receiver of the SAR system

$$P(f) = H(f)R(f) \quad (7)$$

Under the assumption that the time-domain waveform of received pulse $r(t)$ is identical to that of the transmitted signal, $s(t)$, one can put $R(f) = Ae^{j\theta}S(f)$ in (6), where A and θ are the magnitude and phase of the coefficient of backscattering on the radar target. Thus, the frequency-domain expression at the matched filter output can be expressed as,

$$P(f) = |S(f)|^2 Ae^{j\theta} \quad (8)$$

From (7), it is shown that the bandwidth of the processed echo pulse, $p(t)$, at the MF output is the same as that of the transmitted chirped pulse, $s(t)$.

3.2 Conventional Design of MF Receiver Employing Windowing Technique for SAR Pulse Compression

The MF applies the process of FFT to the received SAR signal as already shown in Fig. 2. The application of this process is performed under the assumption that the received signal is periodic, which is not the general case. When the received signal is non-periodic, then the FFT results in a spread of the received signal spectrum (in the frequency domain) that makes the frequency content of the received signal difficult to identify. To deal with this problem, the proposed receiver design employs a time-domain window function that results in a periodic signal when multiplied by the received signal. As a consequence of employing this window, the resulting sidelobes of the signal at the receiver output are suppressed. Matched filtering can be done in the frequency domain, by combining the MF operation with the windowing so that required computation is reduced. Figure 3 shows the block diagram for frequency domain windowing for LFM side lobe suppression. In this diagram it is shown how the window is applied to the filter frequency response before the true filtering step.

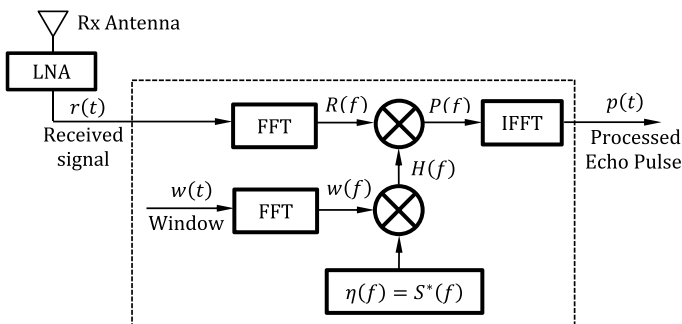


Fig. 3 Block diagram for the conventional software-defined MF receiver employing the conventional windowing technique for improving the performance of radar pulse compression using LFM-chirping

4 Proposed SAR System Receiver with Optimized Compression Window: Novel Design of the MF Receiver

A time-domain window of a standard shape such as Hamming or Hanning or any other standard pulse can be employed in the proposed receiver design. However, it is proposed to construct an optimized window shape by application of the PSO for the purpose of minimizing the SLL of the signal at the receiver output and achieving a specific pulse CR. The proposed windowing method for SAR pulse compression can be explained in view of the block diagram shown in Fig. 4.

In the proposed software-defined transceiver of the SAR whose block diagram is shown in Fig. 3, the transmitted pulse $s(t)$ is obtained by using phase-locked-loop (PLL) that employs a voltage-controlled oscillator (VCO) with saw tooth control input to get the desired frequency ramp form in the time domain with feedback for frequency controlled. The frequency-domain form of the transmitted signal $s(t)$ is obtained by

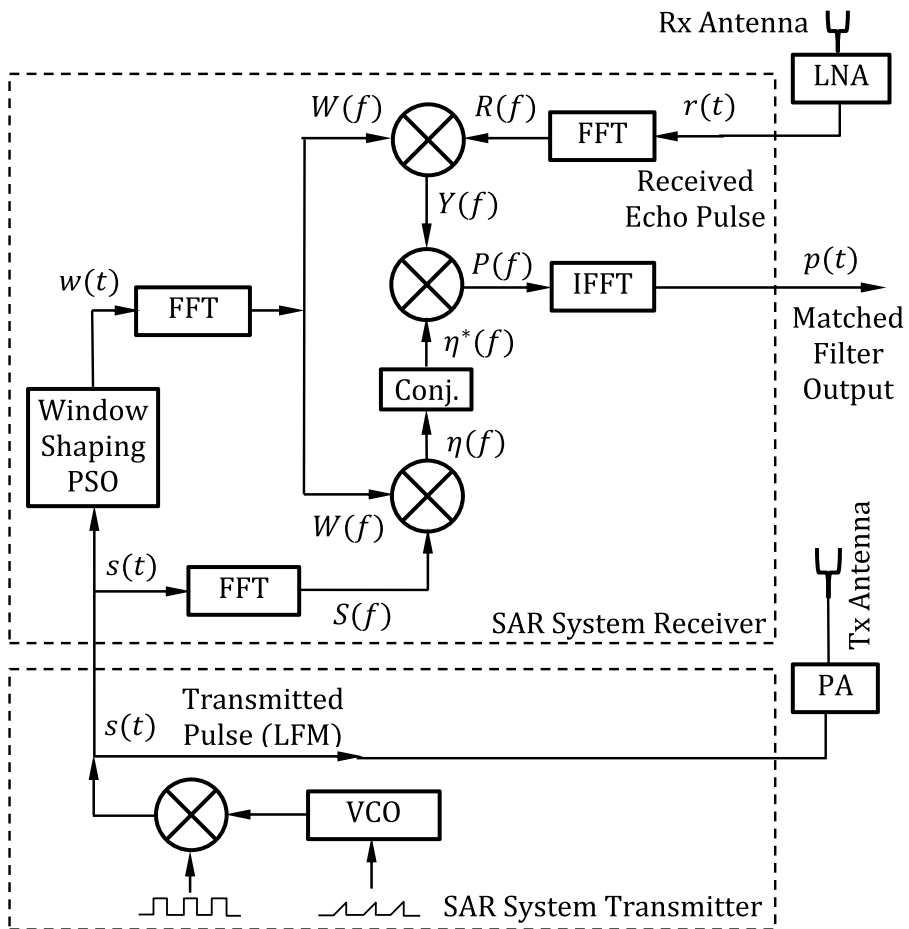


Fig. 4 Block diagram of the proposed software defined MF based on windowing technique for radar pulse compression

the application of FFT and storing the output $S(f)$ in the receiver memory. The time-domain form of the compression window function, $w(t)$, is obtained by applying the PSO as described in following Sections, 5 and 6, of the present paper. The frequency-domain form of the compression window $W(f)$ is obtained by applying FFT to the time-domain form of the window function, $w(t)$.

The transfer function $\eta(f)$ is constructed by multiplying the FFT of the reference (LFM) pulse, $s(t)$, which is the pulse to be transmitted, by $t W(f)$ as follows.

$$\eta(f) = W(f)S(f) \quad (9)$$

The function $R(f)$ is obtained as the FFT of the received echo, $r(t)$ and is, then, multiplied by the FFT, $W(f)$, of the window function to get the frequency domain function $Y(f)$.

$$Y(f) = W(f)R(f) \quad (10)$$

Finally, the function $Y(f)$ is multiplied by the conjugate of the transfer function $\eta(f)$ to get the frequency-domain form the pulse at the output of the SAR receiver, $P(f)$.

$$P(f) = Y(f)\eta^*(f) \quad (11)$$

The function $P(f)$ is then subjected to IFFT to get the received pulse, $p(t)$, at the output of the MF. According to (9) through (11), the spectrum of receiver output can be expressed as follows.

$$P(f) = H(f)R(f) \quad (12)$$

where $H(f)$ is the overall transfer function of the SAR receiver.

Making use of (10) the expression (11) can be reformulated as follows.

$$P(f) = W(f)\eta^*(f)R(f) \quad (13)$$

Making use of (9), the conjugate of $\eta(f)$ can be substituted into the expression (13) to get.

$$P(f) = W(f)W^*(f)S^*(f)R(f) \quad (14)$$

Finally, $P(f)$ can be expressed as follows.

$$P(f) = \left| W(f) \right|^2 \left| S^*(f) R(f) \right| \quad (15)$$

For simulation, it is assumed that the received signal $r(t)$ is identical to the transmit signal, $s(t)$, and hence one can consider $R(f) = Ae^{j\theta}S(f)$ as mentioned above. Under this assumption, the substitution for $R(f)$ into (15) gives following expression for the signal at the MF output.

$$P(f) = |W(f)|^2 |S(f)|^2 Ae^{j\theta} \quad (16)$$

As the window $w(t)$ is a narrow pulse in time domain, it has a wide spectrum $W(f)$ in the frequency domain. Thus, according to (16), the pulse $p(t) = \text{IFFT}\{P(f)\}$ is much narrower than $s(t)$ in the time domain.

5 Optimized Time-Domain Window for SAR Pulse Compression

In this section, the method of compression window optimization to produce minimum SLL for a specific desired value of the pulse CR is described in detail. First, the time-domain window is constructed as piecewise linear curve and then the PSO algorithm is applied after the formulation of the cost function. The following subsections are dedicated for this purpose.

5.1 Piecewise-Linear Segmentation for Construction of the Time Waveform of the Compression Window

To get the optimum shape of the windowing function that minimizes the SLL and achieves a desired value of the pulse CR, this window constructed as successive time samples of arbitrary values as shown in Fig. 5, the compression window can be described as a vector \mathbf{w} , which gives the values of the window at the corresponding times samples given by the time vector \mathbf{t} .

$$\mathbf{w} = [w_1, w_2, \dots, w_n, \dots, w_K] \tag{17}$$

$$\mathbf{t} = [t_1, t_2, \dots, t_n, \dots, t_K] \tag{18}$$

where, K , is the number of time samples.

Also, it is assumed that the interconnections between the sample points of the compression window are straight-line segments. In other words, each pair of successive points (t_{k-1}, w_{k-1}) and (t_k, w_k) are connected by a linear segment. It should be noted that for simulation, the application of the time window starts with the start of the chirped pulse. This

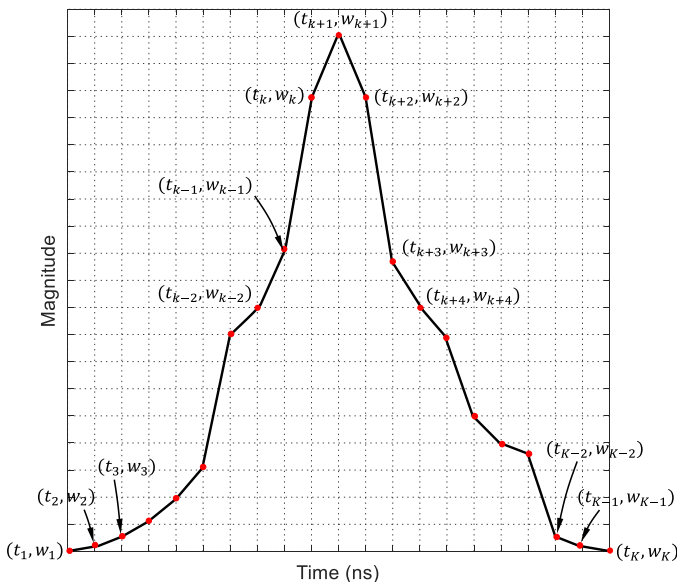


Fig. 5 Piecewise linearly segmented curve for the window function in the time domain

means that the duration of the application of the compression window $w(t)$ is the same as the duration of the SAR pulse. However, the window width can be different from the SAR pulse width. This means that $t_K = T + t_0$ and $K = N_s - N_0$. In general, the compression window can take arbitrary shape. However, the width of $w(t)$ can be given as the 3 dB power width which is the time interval over which the window samples have one-half the total power of the compression window. The width, T_w , of the compression window is defined as the central time duration over which the area under the squared curve is one-half the total area under the squared curve. This time interval is centered at $t_c = \frac{N}{2}\Delta t + t_0$.

5.2 Application of the PSO to Minimize the SLL of the Received Echo Pulse

The objective of the optimization problem is to arrive at the optimal shape of time-domain compression window in its discrete form under the assumption that the discrete points of the window are interconnected using linear segments. The final goal is to minimize the SLL of the SAR pulse at the output of the MF of the SAR receiver and to realize a predetermined value of the CR. The swarm is composed of N_s particles; each particle can be considered as a vector \mathbf{w} has N components (time samples) as given by (20).

5.2.1 Formulation of the Optimization Problem

Let the achieved time duration between the first two nulls on the sides of the main lobe of the signal $r(t)$ at the output of the MF be T_p and let the desired value (optimization goal) of this duration to be T_D . Thus, the target value of CR_D is T/T_D . The CR of the radar pulse is defined as the ratio between the chirped pulse width, T , and the time duration, T_p , between the first nulls on the sides of the main lobe of the compressed pulse at the receiver output. Thus, the achieved CR can be defined as $CR = CR_p = T/T_p$. As the objective of the PSO algorithm is to minimize the SLL and to get the compressed pulse width, T_p , as close as possible to the desired width, T_D , the cost function can be formulated as follows.

$$\mathcal{C}(\mathbf{w}) = F_S \ell_{\max}(\mathbf{w}) + F_P |T_p(\mathbf{w}) - T_D| \quad (19)$$

where $\ell_{\max}(\mathbf{w})$, is the maximum SLL achieved by a window shape that is given by the vector \mathbf{w} , $T_p(\mathbf{w})$ is the achieved width, T_D is the desired pulse width, F_S and F_P are weighting factors to determine the contributions of the maximum SLL and the deviation from the desired window width to the cost function $\mathcal{C}(\mathbf{w})$.

According to (19), the PSO has two objectives; minimization of the maximum SLL and achieving a predetermined value of the pulse CR. It may be logic to intuit that relaxing the condition to achieve the desired pulse CR enables the PSO algorithm to achieve a lower value of the maximum SLL whereas aiming at a higher CR will cause the achievable SLL to increase.

The optimization problem can be formulated as follows. It is required to get the samples \mathbf{w} that achieve the following

$$\text{minimize } F_S \ell_{\max}(\mathbf{w}) + F_P |T_p(\mathbf{w}) - T_D| \quad (20a)$$

$$\text{subject to } : w_k \geq 0, \forall k \in \{1, 2, \dots, K\} \quad (20b)$$

The constraint (20-b) means the window samples should be positive while the PSO iterations are running.

5.2.2 Implementation of the PSO

The optimization space (swarm of particles and their positions) contains N_p particles. The n th particle has its position within the swarm in the τ th iteration given by the vector $\mathbf{w}_n^{(\tau)}$. The implementation of the PSO algorithm can be divided into four stages: (i) initialization of positions, $\mathbf{x}_n^{(0)}$ and velocities, $\mathbf{v}_n^{(0)}$, for the particles of the swarm. The initial values of the particles $w_n^{(0)}$ where $\forall n \in \{1, 2, \dots, N_s\}$ can be set by assigning the sample values of $W_{n,k}^{(0)}$ to take the shape of Hamming window with the width, W_H . The samples of

$$w_{n,k}^{(0)} = w_k^{(H)} * [1 + 0.1(r_{n,k} - 0.5)] \tag{21}$$

where k is the time sample index, n is the particle number, and $r_{n,k}$ is a random $\in [0, 1]$. The subscripts n, k of the $r_{n,k}$ mean that this random number is generated for each pair of the indices (n, k) . (ii) calculation of the local best positions, \mathbf{y}_n , for the particles, (iii) Calculation of the global best position, \mathbf{g} , (iv) calculation of the particles velocities, $\mathbf{v}_n^{(1)}$, and positions, $\mathbf{x}_n^{(1)}$, for the next iteration. The superscript^(H) refers to the samples of the Hanning window that is suggested as the initial values of the window samples.

The following equations are used to implement an iterative PSO algorithm:

$$\mathbf{v}_n^{(\tau)} = u\mathbf{v}_n^{(\tau-1)} + c_1r_1[\mathbf{y}_n^{(\tau-1)} - \mathbf{x}_n^{(\tau-1)}] + c_2r_2[\mathbf{g}^{(\tau-1)} - \mathbf{x}_n^{(\tau-1)}] \tag{22a}$$

$$\mathbf{x}_n^{(\tau)} = \mathbf{x}_n^{(\tau-1)} + \mathbf{v}_n^{(\tau)} \tag{22b}$$

where τ is the iteration number (time index), u is the inertia weight parameter, c_1, c_2 are acceleration factors and r_1, r_2 are random numbers between 0 and 1. For each particle, the initial position, $\mathbf{x}_n^{(0)}$, is determined by assigning random values (varying around the unity) to the amplitudes of the excitation voltages of the array elements. The initial local best position of each particle, $\mathbf{y}_n^{(0)}$, is assigned the same initial value of the particle position, $\mathbf{x}_n^{(0)}$. The initial value of the velocity of each particle is set to zero. The local best position, $\mathbf{y}_n^{(\tau)}$, for each particle is the position of this particle that results in the minimum value of the cost function over the progressive iterations during the run of the PSO algorithm. The global best position, $\mathbf{g}^{(\tau)}$, for the particles in the swarm is the position among the local best positions that results in the absolute minimum value of the cost function over the successive iterations during the run of the PSO algorithm. In each iteration, the velocity, \mathbf{v}_n , and position, \mathbf{x}_n , for each particle in the swarm are updated, as given by (22-a) and (22-b).

6 Results and Discussions

This section is concerned with the presentation and discussion of the numerical results of the achieved SLL and pulse CR using the conventional LFM chirping and the conventional weighting window methods. Also various the achievements of SAR pulse compression techniques proposed in some recent publications. Finally the SLL and pulse CR achieved by the optimized window technique introduced in the present work

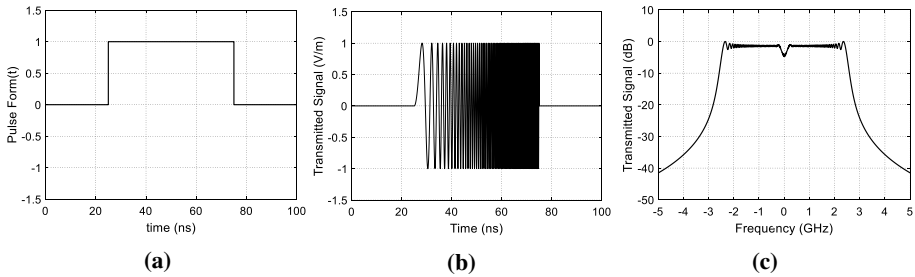
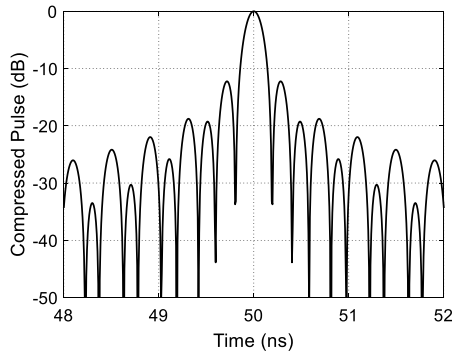


Fig. 6 The chirped pulse using the conventional LFM: **a** Square pulse before chirping (a) time-domain form of the chirped pulse, $s(t)$. **b** Frequency-domain form of the chirped pulse $S(f)$

Fig. 7 Time waveform of the compressed pulse at the output of the MF with maximum SLL of about -13.1 dB and pulse CR of about 128



are presented, discussed, and compared to those achievement available in the most recently published work.

6.1 Chirped SAR Pulse using Conventional LFM

The LFM is a conventional method for improving the resolution of the radar, the unchirped radar pulse, shown in Fig. 6a is subjected to chirping using LFM. Thus, the square pulse becomes the envelope of a sinusoidal wave whose instantaneous frequency increases linearly with time as shown in Fig. 6b. It is shown that the phase of the sinusoidal signal is zero at the start time of the chirped pulse. A numerical example can be used for quantitative explanation; a square pulse of duration $T = 50$ ns, Fig. 6a is subjected to chirping using LFM as described in Sect. 2 to get the chirped pulse whose time waveform is shown in Fig. 6b. For discretization, the sampling frequency is set as $f_s = 15f_c$, where $f_c = 1.27$ GHz is the central frequency, $N_s = 15$, and $L = 12700$. The application of the FFT results in the frequency spectrum of the chirped pulse shown in Fig. 6c.

The process of the conventional MF described in Sect. 3 is applied to receive and process the echo pulse, $r(t)$, reflected from the radar target due to the transmitted chirped pulse, $s(t)$, described above. The time waveform of the conventionally LFM-chirped pulse at the receiver MF output is shown in Fig. 7. It is shown that the processed echo pulse, $p(t)$, at the MF output has a main lobe and many side lobes of very low level relative to that of the main lobe. The main lobe is compressed, i.e., it has very short time duration relative to the duration T of the transmitted radar pulse. However, many side lobes exist, the highest

of them is the second lobe. It shown that the maximum SLL is about -13.1 dB. The width of the pulse $p(t)$ can be calculated as the time difference between the first two nulls on the sides of the main lobe. It is shown that the compressed pulse width is 0.39 ns. The pulse compression can be obtained by dividing the width of the pulse before compression, Fig. 6a by the width of the main lobe of $p(t)$; this gives a CR of 128. Thus, the frequency chirping using LFM results in very high CR but such SLL may not be adequate for accurate SAR imaging.

6.2 Compression Window Technique to Improve the Performance of LFM-Chirping

As mentioned in Sect. 4, the application of time or frequency windowing to LFM-chirped pulse leads to improve the performance of the pulse compression regarding the CR and the maximum SLL. One of the well-known and most effective time-domain windows is the Hanning window. The application of Hanning window of width 1 ns, shown in Fig. 8a, to the LFM-chirped pulse, shown in Fig. 6, results in the time waveform shown in Fig. 8b for the received signal at the output of the MF. The width of the main lobe is 1.2 ns, which corresponds to CR of about 42, whereas the maximum SLL is about -22.6 dB.

For investigating the impact of the compression window width on the effectiveness of the proposed pulse compression process, the following example is demonstrated. In this example, the application of Hanning window of width 6 ns, whose time waveform is presented in Fig. 9a, results in the received signal at the output of the MF whose time waveform is shown in Fig. 9b. It is shown that the width of the main lobe is 6.6 ns, which corresponds to CR of about 7.5, whereas the maximum SLL is about -28.2 dB.

From the previous two examples, it is clear that to obtain lower SLL of the received pulse at the MF output, the width of the Hanning window should be increased which, in turn, results in lower CR of the SAR pulse. Thus, a compromise should be done to choose the window width that is more appropriate for a specific application.

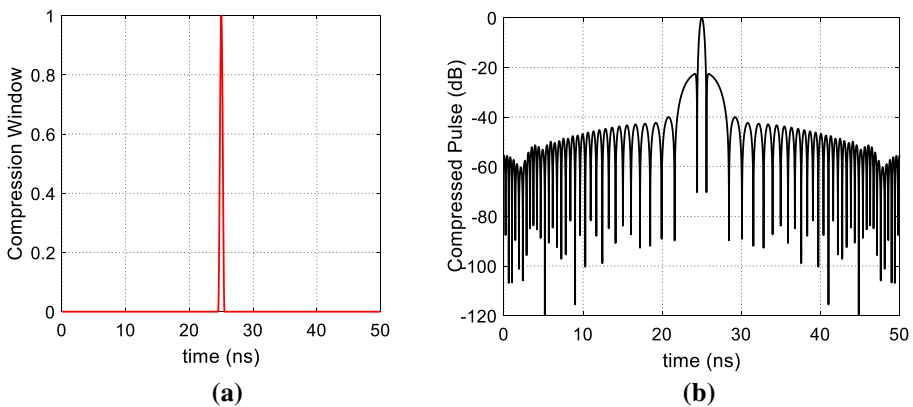


Fig. 8 The Hanning window of width = 1 ns leads to compressed pulse with maximum SLL of about -22.6 dB and pulse CR of about 42. **a** Compression window. **b** Compressed pulse at the output of the MF

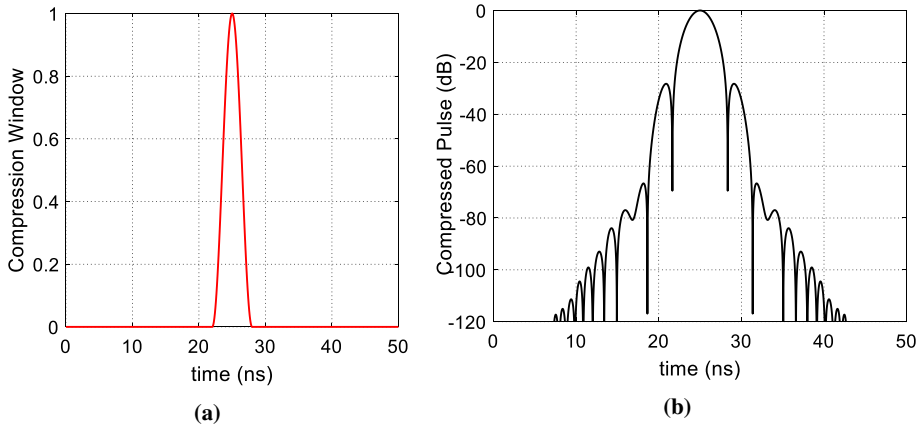


Fig. 9 The Hanning window of width = 6ns leads to compressed pulse with maximum SLL of about -28.2 dB and pulse CR of about 7.4. **a** Compression window. **b** Compressed pulse at the output of the MF

6.3 The Optimized Window for SAR Pulse Compression

In this subsection, six numerical examples are presented to show the performance of SAR pulse compression using the optimized window technique proposed in the present work.

The PSO algorithm runs to construct the optimum window with the optimization goal to achieve a predetermined value of the CR and to minimize the SLL. Let the initial window shape for the PSO algorithm be that of a Hanning window of width 1ns as that shown in Fig. 10a. In this case, the PSO algorithm takes about 300 iterations to arrive at the optimized window shape shown in Fig. 10b whose width is still 1ns like that of the initial window. The resulting time waveform of the compressed pulse at the MF output is shown

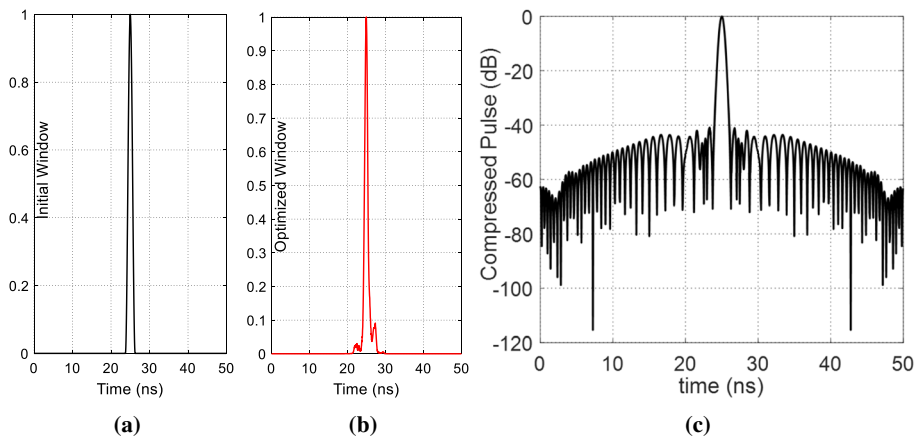


Fig. 10 The optimized window of width = 1ns leads to a compressed pulse with maximum SLL of about -40.5 dB and pulse CR of about 20. **a** Initial window. **b** Optimized window. **c** Compressed pulse at the output of the MF

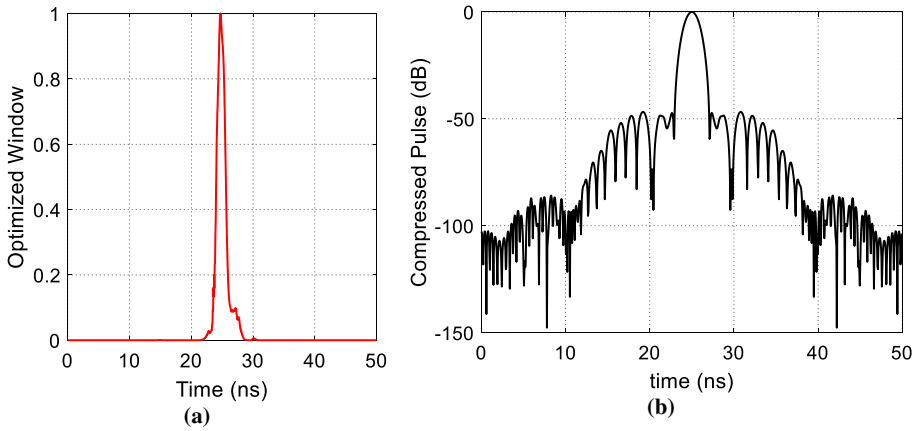


Fig. 11 The optimized window of width = 1.68ns leads to a compressed pulse with maximum SLL of about -45dB and pulse CR of about 12. **a** Optimized window. **b** Compressed pulse at the output of the MF

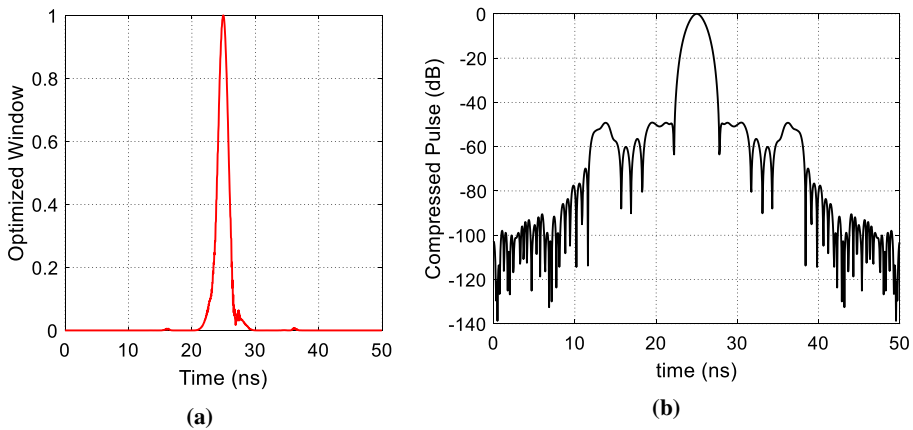


Fig. 12 The optimized window of width 2.32ns leads to a compressed pulse with maximum SLL of about -49dB and pulse CR of about 9. **a** Optimized window. **b** Compressed pulse at the output of the MF

in Fig. 10c where the main lobe width is about 2.5ns. The resulting CR is 20, whereas the maximum SLL is about -40.5dB. Thus, when compared with the case of applying the Hanning window of width 1ns as previously discussed; see Fig. 8, the application of an optimized window of the same width results in reducing the SLL from -22.6dB to -40.5dB whereas the CR is decreased from 42 to 20. As the SLL is more critical for the radar operation than the CR, the application of the optimized window can be considered much superior to the application of the Hanning window.

Other cases are for compressed pulse using the optimized window present in Figs. 11, 12, 13 and 14. In these examples, it is shown that the lower the predetermined (desired) pulse CR the lower the achieved SLL.

The last example of the application of PSO on Hanning window is shown in Fig. 15 with width 6ns. The optimized window shape is shown in Fig. 15a. The output of the MF is

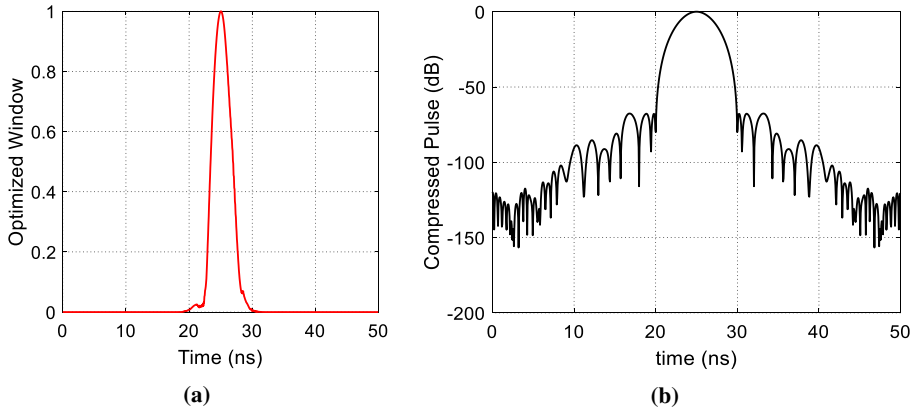


Fig. 13 The optimized window of width 2.9ns leads to a compressed pulse with maximum SLL of about -63 dB and pulse CR of about 5. **a** Optimized window. **b** Compressed pulse at the output of the MF

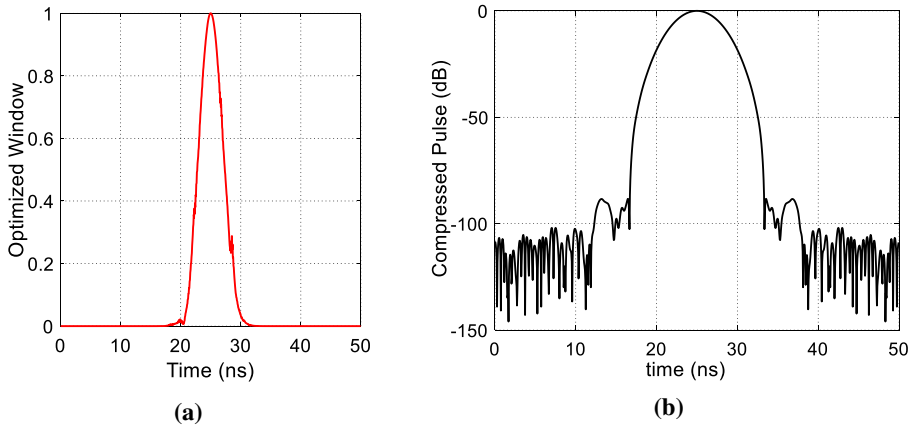


Fig. 14 The optimized window of width 4.5ns leads to compressed pulse with maximum SLL of about -88 dB and pulse CR of about 3. **a** Optimized window. **b** Compressed pulse at the output of the MF

the time waveform of the compressed pulse shown in Fig. 15b where the main lobe width is about 25ns. The resulting CR is 2, whereas the maximum SLL is -115 dB. Thus, when compared with the case of applying the Hanning window of width 6ns, the application of the optimized window of the same width results in reducing the SLL from -28.2 dB to -114 dB whereas the CR is decreased from 7.4 to 2.

For comparative assessment of the effectiveness of the proposed method, the well known Hanning window, as one of the conventional time-domain shapes of the radar pulse compression windows, is applied to compress the SAR pulses presented in Fig. 6. so as to compare its performance regarding the resulting pulse CR and maximum SLL with the performance obtained by the application of the optimized window proposed in the present work. A Matlab® is written specially for the purpose of comparison. It should be noted that some results that have been obtained by applying the Hanning window are presented in Figs. 8 and 9. Table 1 shows a list of the achieved SLL and the

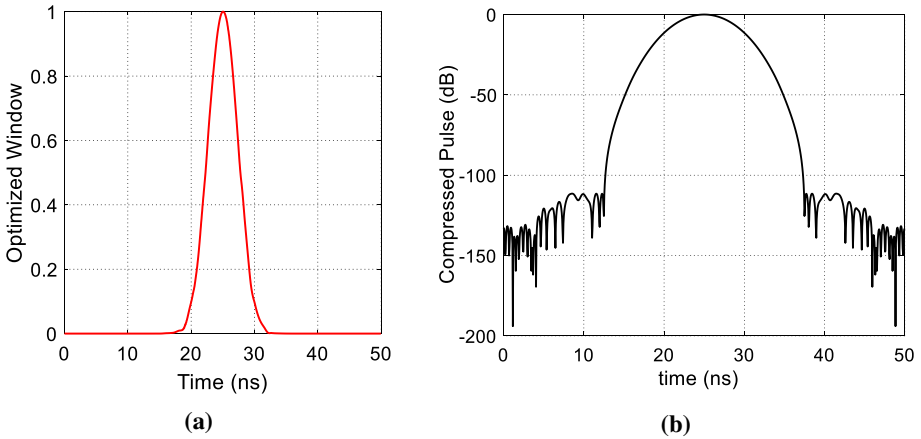


Fig. 15 The optimized window of width = 6ns leads to a compressed pulse with maximum SLL of about -114dB and pulse CR of about 2. **a** Optimized window. **b** Compressed pulse at the output of the MF

Table 1 The achieved SLL and pulse CR in comparison to the corresponding values achieved by Hanning window

CR		40	20	12	10	8	7	6	5	4	3	2	1.5
SLL	Hanning	-23	-23.5	-24	-25	-27	-30	-32	-36	-41	-49	-60	-70
	Proposed	-30	-42	-44	-46	-51	-55	-58	-65	-71	-90	-114	-133

corresponding CR using the Hanning window compared to those achieved by the optimized window technique proposed in the present work. It is shown that, for the same value of the pulse CR, the proposed window achieves much lower value of the SLL than that achieved by the Hanning window. It should be noted that, a narrower compression window gives higher pulse CR. For example, for a pulse CR of 20, Hanning window of width 1ns achieves a SLL of -23.5dB , whereas the proposed window (of the same width) achieves a SLL of -42dB . For relatively low pulse CR of 5, Hanning window of width 5.2ns achieves a SLL of -36dB , whereas an optimized window of the same width achieves a SLL of -65dB . Thus, with increasing the compression window width the maximum SLL is improved whereas pulse CR is decreased. However, the rate of reduction (improvement) of the SLL with increasing the width of the compression window using the proposed optimized window is much better than that obtained by the application of Hanning window provided that both windows have the same width.

6.4 Relations Among the Achieved CR, SLL and Width of the Compression Window

Two objectives are to be achieved Predetermined value of the CR and low SLL of the received SAR pulse at the MF output. Figure 16 presents the dependencies of the max SLL of the received pulse at the MF output and the corresponding CR on the width of

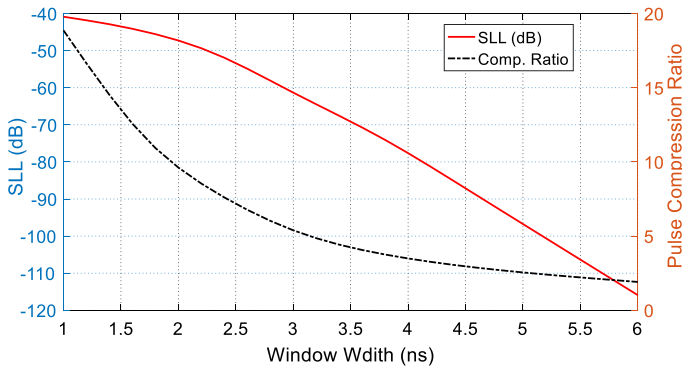


Fig. 16 Dependence of the achieved SLL and pulse CR of the resulting compressed pulse on the width of the window after the application of the PSO

the compression window that has been optimized using the PSO. It is shown that to obtain lower SLL of the received pulse at the MF output the width of compression window should be increased which results in lower CR of the SAR pulse. Thus, the objectives of high CR and low SLL seem to be contradicting with each other. A compromise should be carried out to select the optimum width of the compression window.

6.5 Computational Efficiency and Rate of Convergence of the PSO Algorithm

The cost function $\mathcal{C}(\mathbf{w})$ given by (19) decays with progressive iteration of the PSO algorithm as shown in Fig. 17 for three different cases. As shown in this figure, the PSO consumes from 200 – 400 iterations to reach the steady state at which the best achievable performance is obtained. The stair case in the curve is attributed to the application of the constraint given by (20-b). In each iteration, if a time sample of the compression window is negative it is overridden to be zero. Of course, the application of this constraint causes the decay curve to be locally horizontal which results in the staircase

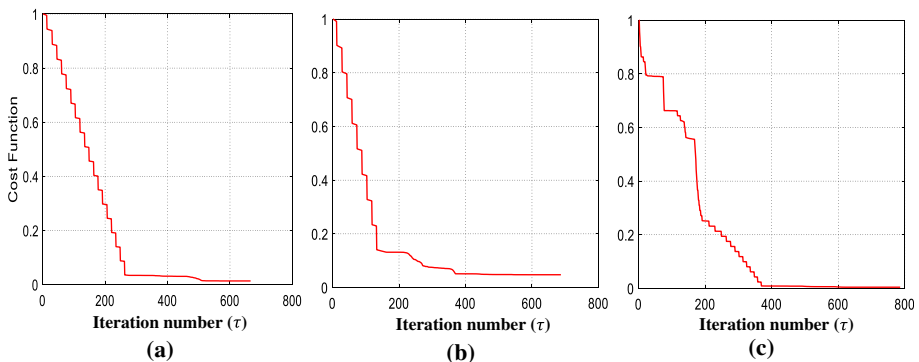


Fig. 17 Decay of the cost function with the successive iterations of the PSO algorithm. **a** CR=7, SLL=-54dB. **b** CR=8, SLL=-51dB. **c** CR=9, SLL=-49dB

appearance of the curve and also, slows down the decay of the cost function with the PSO iterations.

The fast convergence of the PSO algorithm and the low value of the cost function at the steady state of the PSO algorithm reflects the computational efficiency of the proposed method including the suitable formation of the optimization problem together with the cost function and the robustness of the developed algorithm for the application of the PSO.

6.6 Comparative Performance Summary

Comparisons among the achieved SLL using different pulse compression techniques proposed in some recent publications are demonstrated in Table 2. It is shown that the optimized compression window method proposed in the present work gives much lower SLL than those obtained in the other published work. However, the achieved SLL in the present work is variable and depends on the desired value of the pulse CR as listed in Table 2. It should be noted that the methods listed in Table 2 are briefly mentioned in the “Introduction” section of the present paper. Also, it is noticed that the best results considering the suppression of the sidelobes result in SLLs of those obtained using the methods that employ combined techniques like those presented in [15] and [16] to obtain SLLs of about -49dB and -62dB , respectively. Recall that the method presented in [15], applies the combined spectrum modification and window weighting technique for SAR pulse compression, whereas the work of [16] introduces the combined technique of phase predistortion and spectrum modification for SAR pulse compression. However, the maximum SLLs achieved in the present work depend on the pulse CR. To achieve better SLL, the pulse CR should be reduced. As shown in Table 1, a maximum SLL of -65dB is achieved for pulse CR of 5, which is better than those obtained in [15] and [16].

7 Conclusion

A novel design of a software-defined filter for digital receivers of SAR systems has been proposed. The proposed filter produces a SAR pulse with higher CR and lower SLL than that produced by the conventional MF. The novel filter design is based on the time windowing of the SAR pulse, where the shape of the proposed time-domain window is optimized to minimize the SLL and to realize the desired pulse CR. The transmitted SAR pulse is, first, subjected to LFM and then subjected to the optimized window. The proposed window is constructed as a sequential continuous piecewise linear segments. The PSO algorithm is then applied to get the window shape that minimizes the SLL for a specific predetermined value of the pulse CR. The iterative PSO is shown to be fastly convergent and computationally efficient. Also, it is shown that the desired value of the pulse CR is exactly achieved. On the other hand, the achieved SLLs are about -65 dB , -90 dB , -114 dB , and -133 dB for pulse CRs of 5, 3, 2, and 1.5, respectively. By comparison, the method proposed in the present work has been proved to be superior to those conventional windowing techniques used for radar pulse compression. For example, a pulse CR of 20, Hanning window of width 1ns achieves a SLL of -23.5dB , whereas the proposed window achieves a SLL of -42dB . For relatively low pulse CR of 5, Hanning window of width 5.2ns achieves a SLL of -36dB , whereas an optimized window of the same width achieves a SLL of -65dB . Als,

Table 2 Comparisons among the achieved SLL due to the application of SAR pulse compression techniques available in some publications and the SLL achieved in the present work

Compression method	Achieved SLL
[13] Stretch and Correlation, 2020	-23.8dB
[9] Temporal Predistortion, 2014	-40dB
[10] Modified Tapered Window, 2021	-43dB
[11] NLFM, Stationary Phase Technique, 2014	-47.3dB
[15] Spectrum Modification and Windowing, 2012	-49dB
[16] Phase Predistortion and Spectrum Modification, 2013	-62dB
	Achieved SLL
Method proposed in the present work	
CR	
5	-65dB
4	-71dB
3	-88dB
2	-114dB
1.5	-133dB

when compared with the numerical results presented in some recently published work, the SLL achieved in the present work for specific pulse CR is shown to be better than those than those obtained by the other techniques. As the proposed technique has been applied in the present paper for only LFM chirped pulse, it is suggested, as a future extension, to apply the optimized window technique, for compression of a SAR pulse that has been chirped using NLFM. This is expected to give better performance of the SAR pulse compression than that obtained using LFM chirping.

Funding Open access funding provided by The Science, Technology & Innovation Funding Authority (STDF) in cooperation with The Egyptian Knowledge Bank (EKB). Funding not applicable to this article (no funds for this research).

Data Availability Data sharing not applicable to this article as no datasets were generated or analyzed during the current study. Availability of data and material not applicable as there is no data sets used.

Code Availability Code availability not applicable, no codes developed in this research.

Declarations

Conflict of interest Authors declare that there are no Conflicts of interest for this research.

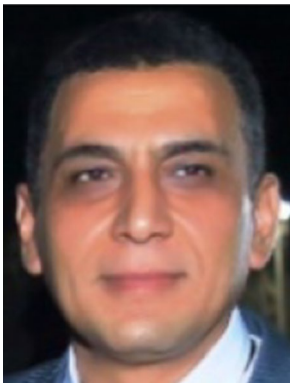
Open Access This article is licensed under a Creative Commons Attribution 4.0 International License, which permits use, sharing, adaptation, distribution and reproduction in any medium or format, as long as you give appropriate credit to the original author(s) and the source, provide a link to the Creative Commons licence, and indicate if changes were made. The images or other third party material in this article are included in the article's Creative Commons licence, unless indicated otherwise in a credit line to the material. If material is not included in the article's Creative Commons licence and your intended use is not permitted by statutory regulation or exceeds the permitted use, you will need to obtain permission directly from the copyright holder. To view a copy of this licence, visit <http://creativecommons.org/licenses/by/4.0/>.

References

1. Zhou, Y., Wang, W., Chen, Z., Zhao, Q., Zhang, H., Deng, Y., & Wang, R. (2021). High-resolution and wide-swath SAR imaging mode using frequency diverse planar array. *IEEE Geoscience and Remote Sensing Letters*, *18*(2), 321–325.
2. Wei, S., Zeng, X., Qu, Q., Wang, M., Su, H., & Shi, J. (2020). HRSID: A high-resolution SAR images dataset for ship detection and instance segmentation. *IEEE Access*, *8*, 120234–120254.
3. Soliman, S. A. M., Hussein, K. F. A., & Ammar, A. E. H. A. (2021). Electromagnetic simulation for estimation of forest vertical structure using PolSAR data. *Progress In Electromagnetics Research*, *90*, 129–150.
4. Soliman, S. A. M., Hussein, K. F. A., & Ammar, A. E. H. A. (2020). Electromagnetic resonances of natural grasslands and their effects on radar vegetation index. *Progress In Electromagnetics Research B*, *86*, 19–38.
5. Kumar, A., Nidhi, M. (2015). Radar pulse compression technique for linear frequency modulated pulses. *International Journal of Engineering and Technical Research (IJETR)*, *3*(8), 2454–4698. ISSN: 2321–0869.
6. Likhith Reddy, D., Subba Rao, S.V. (2019). A novel design of matched filter for digital receivers. *International Journal of Recent Technology and Engineering (IJRTE)*, *8*(3). ISSN: 2277–3878.
7. Chan, Y. K., Chung, B.-K., & Chuah, H.-T. (2004). Transmitter and receiver design of an experimental airborne synthetic aperture radar sensor. *Progress In Electromagnetics Research*, *49*, 203–218.
8. Grabowski, A. SDR-based LFM signal generator for radar/SAR systems. In *2016 17th International Radar Symposium (IRS)* (pp. 1–3), IEEE, 2016.
9. Vizitiu, I. C. (2014). Some aspects of sidelobe reduction in pulse compression radars using NLFM signal processing. *Progress In Electromagnetics Research C*, *47*, 119–129.
10. Volodymyr, G. (2021). On application of taper windows for sidelobe suppression in LFM pulse compression. *Progress In Electromagnetics Research C*, *107*, 259–271.

11. Vizitiu, I.-C., Enache, F., & Popescu, F. (2014). Sidelobe reduction in pulse-compression radar using the stationary phase technique: An extended comparative study. In *2014 International Conference on Optimization of Electrical and Electronic Equipment (OPTIM)*, pp. 898–901. IEEE.
12. El_Mashade, M. B., Akah, H., & El-Monem, S. A. (2020) Windowing accuracy evaluation for PSLR enhancement of SAR image recovery. *Advances in Science, Technology and Engineering Systems Journal*, 5(1), 48–57.
13. Ashry, M. M., Mashaly, A. S., & Sheta, B. I. (2020). Comparative analysis between SAR pulse compression techniques. In *2020 12th International Conference on Electrical Engineering (ICEENG)* (pp. 234–240), IEEE, 2020.
14. Dominguez, E.M., Magnard, C., Frioud, M., Small, D. & Meier, E. (2017). Adaptive pulse compression for range focusing in SAR imagery. *IEEE Transactions on Geoscience and Remote Sensing*, 55(4), .2262–2275 .
15. Lin, K., 2012, December. Pulse Compression Using Spectrum Modification and Window Weighting Techniques. In *2012 International Conference on Control Engineering and Communication Technology* (pp. 133–136). IEEE.
16. Wang, H., Shi, Z., & He, J. (2013). Compression with considerable sidelobe suppression effect in weather radar. *EURASIP Journal on Wireless Communications and Networking*, 2013(1), 1–8.
17. Wang, D., Tan, D., & Liu, L. (2017). *Particle swarm optimization algorithm: An overview*". Springer.

Publisher's Note Springer Nature remains neutral with regard to jurisdictional claims in published maps and institutional affiliations.



Khalid. F. A. Hussein received his B.Sc., M.Sc. and Ph.D. degrees in the Department of Electronics and Electrical Communications, Faculty of Engineering, Cairo University, 1990, 1995 and 2001, respectively. He is currently a professor at the Department of Microwave Engineering at the Electronics Research Institute. He has work experience in scientific research for more than 29 years. He has teaching experience in engineering colleges in many universities for more than 20 years. He has supervised more than seventy doctoral and master theses. He has published more than 100 papers in international, regional and local scientific journals and conferences. He has served as Head of Microwave Engineering Department at the Electronics Research Institute for up to four years. He has been a member of the Egyptian Space Program (currently the Egyptian Space Agency) for more than eight years. He has worked as Principal Investigator for four research projects and Head of Research Group in four other research projects. He designed and implemented several satellite antennas between prototypes and finished products. He has provided scientific consultations and conducted

field measurements related to the design and distribution of mobile communication base station antennas for good signal coverage in behalf of many Egyptian and international companies. His research interests are in the areas of antennas, electromagnetic wave propagation, risk assessment of human exposure to microwave radiation, optical communications, photonics, quantum computing, radar systems, particularly ground penetrating radar (GPR), synthetic aperture radar (SAR), and remote sensing systems.




Asmaa O. Helmy was born in Egypt in 1989. She received the B.Sc. degree in electronics and communications from Zagazig Faculty of Engineering in 2011 and the M.Sc. degree in 2015 from Zagazig University, Egypt. She is currently a teaching assistant at Higher Institute of Electronic Engineering in Belbeis, Egypt and pursuing the Ph.D. degree. Her current research interest in Transceiver of Synthetic Aperture Radar for Earth Remote Sensing.



Ashraf S. Mohra was born in Egypt in 1963. He received the B.Sc. degree in Electronics and communications from Shoubra Faculty of Engineering in 1986. He received the M.Sc. and Ph.D. degree in Electronics and communications from Ain Shams University, Cairo, Egypt, in 1994 and 2000, respectively. He is currently professor of Electrical Engineering, at Benha Faculty of Engineering, Benha University, Egypt. His current research interests include microstrip antennas, filters, couplers, Hybrid junctions, computer aided design of planar and uniplanar of MIC's and MMIC's, Non-destructive techniques, Meta-materials and defected ground structure.

Authors and Affiliations

Khalid F. A. Hussein¹  · Asmaa O. Helmy³ · Ashraf S. Mohra²

Asmaa O. Helmy
asmaa.helmy792@yahoo.com

Ashraf S. Mohra
amohra@bhit.bu.edu.eg

¹ Electronics Research Institute (ERI), Cairo 11843, Egypt

² Department of Electrical Engineering, Faculty of Engineering, University of Benha, Benha, Egypt

³ Department of Electronics and Communications, High Institute of Electronic Engineering, Ministry of Higher Education, Bilbis-Sharqia 44621, Egypt